LOAD SEPARATION PRINCIPLE IN DETERMINATION OF *J-R* CURVE FOR DUCTILE POLYMERS: SUITABILITY OF DIFFERENT MATERIAL DEFORMATION FUNCTIONS USED IN THE NORMALIZATION METHOD

Celina Bernal[1], Marta Rink[2], Patricia Frontini[1]*

[1] Institute of Materials Science and Technology (INTEMA), University of Mar del Plata and National Research Council (CONICET), 7600 Mar del Plata, Argentina

[2] Politecnico di Milano, Piazza Leonardo da Vinci 32, 20133 Milano, Italy

SUMMARY: The load separation principle states that the load, *P*, can be represented as the multiplication of two independent functions: a crack geometry function, *G(a)*, and a material deformation function, *H(v)*. The principle constitutes the theoretical basis for the single-specimen *J*-integral experiment and the incremental calculation of *J*-integral crack growth resistance (*J-R*) curves. The normalization method is a new method, which assumes load separation and uses characteristic deformation properties of materials to relate load, displacement and crack length in a functional form. From the deformation material function or "material key curve", *J-R* curve can be developed from a single precracking experiment. This investigation deals with the applicability of the load separation criterion to evaluation of ductile fracture mechanics parameters in rubber-modified polystyrene, polypropylene, rubber-modified PMMA, ABS resin and high-density polyethylene in the bending configuration. Different mathematical relationships for the deformation function (power law function, LMN function and combined power law straight line relationship) have been proposed and compared. The resulting *J-R* curves are in good agreement with those obtained by the traditional multiple-specimen technique. The results presented here imply that the use of a single load-displacement method for evaluation of *J*-integrals for ductile polymers is possible and hence also the normalization method can be used for evaluation of *J-R* curves from a single-test record.

Introduction

Single-specimen methods called normalization methods have been developed for fracture characterization of steels; they allow to calculate the *J-R* curve from a single specimen without the need of an on-line monitoring system like the elastic compliance method used in the ASTM E-1152 *J-R* curve test standard[1,2]. These methods use the deformational characteristic properties of materials relating in a functional form load, displacement and crack length.

The polymer community has also adopted these simple methods capable of determining the *J-R* curve directly from load displacement records[3-6]. There are also obvious merits in being able to obtain *J-R* curves from load, load-point displacement and crack

 CCC 1022-1360/99/$ 17.50+.50/0

extension measurements using a single laboratory specimen. Normalization methods appear to be very promising in the polymer field since they do not need expensive automatic methods for measuring the crack advance and use only one load-displacement record. The application of the unloading compliance method and the indirect electric potential drop method[7], so popular in the *J-R* steel evaluation, even if possible, is more complicated for polymers because of the presence of viscoelastic hysteresis loops[8,9] and the need of instrumentating the sample. The normalization assumes the validity of the load separation principle[2] stated by Ernst[10,11], which implies that for a certain material, geometry and constraint, the load in a load *vs.* displacement record can be represented[2] as separable multiplicative functions of crack length, a, and displacement, v. The load separation is implicit in the analysis of Rice[12] and has been analytically demonstrated for Ramberg-Osgood materials by the EPRI Handbook solutions[13]. In addition, it has been recently experimentally investigated on some configurations and materials[3,4,14].

The normalization method uses the plastic deformation behaviour of the material to infer the crack extension. That is to say, if an appropriate material deformation relationship is known for a material, the crack length can be directly estimated from the corresponding load and displacement values.

Several functions were previously assumed in steel fracture characterization[6,15,16]. So far, two functional forms have been tried in the polymer field: a simple power law[3,5] and the three-parameter LMN equation[4,6,17]. The power law was proposed due to its simplicity and the LMN functional form because it is said to be capable of fitting behaviours[6,18] of most material types.

The success of this method is directly related to the real ability of the mathematical relationship assumed to well represent the deformation characteristics of the material. Hence, this paper aims to compare the advantages and the accuracy of different deformation relationships in evaluating the ductile fracture of polymers.

The reliability of *J-R* curves was verified by contrasting them with a calibration *J-R* curve obtained by the multiple-specimen technique.

Load separation analysis

The evaluation of the material fracture toughness by the *J*-integral, originally defined as a path-independent two-dimensional line integral[12], may be done through the alternative generalized form in terms of energy[19,20]:

$$J = \eta_{el} \frac{A_{el}}{B(W-a)} + \eta_{pl} \frac{A_{pl}}{B(W-a)} \qquad (1)$$

where A_{el} and A_{pl} are the elastic and plastic parts of the area under the load-displacement record. The load separation principle[21] is implicit in this expression.

The load separation principle implies that for a certain material, geometry and

$$P = G\left(\frac{a}{W}\right).H\left(\frac{v_{pl}}{W}\right) \tag{2}$$

where a is the crack length, v_{pl} is the plastic displacement (both normalized by the specimen width W), $G(a/W)$ is the crack geometry function. Being only a function of $G(a/W)$ and $H(v_{pl}/W)$, it represents the deformation character of the material or key curve. It is only a function of the normalized plastic displacement.

It has been demonstrated that the load separation and the v_{pl} range of separability can be determined from two test records P-v_{pl} of different stationary crack lengths (U-notched specimens) a_i and a_j by calculating a separation parameter (S_{ij}) (Eq. (3)) at constant plastic displacement. S_{ij} will have a constant value over the whole domain of the plastic displacement since the geometry function is constant for stationary cracks, and the deformation function is only a function of v_{pl}:

$$S_{ij} = \left.\frac{P(a_i)}{P(a_j)}\right|_{v_{pl}} \tag{3}$$

The constancy of S_{ij} implies that over the whole domain of v_{pl}, the load can be represented by a separable form. The validity of load separation in stationary and growing crack experiments has been verified for many polymers[3,4,14] following procedures first developed for steel evaluation[2,22]. Sharobeam and Landes[22] proved that the load separation can be extended to precracked specimen records if the crack starts to grow beyond the unseparable region, i.e., the load separation assumption during the stable propagation stage controlled by J is only valid for the entire plastic region except for a limited region at the early region of plastic behaviour. The v_{pl} range of load separation validity can be determined by testing a precracked specimen and a U-notched specimen with crack lengths a_i and a_j and by calculating the new separation parameter[3,14] S^{pb}_{ij} where the superscripts p and b denote precracked specimen and blunt-notched (or stationary crack) specimens, respectively:

$$S^{pb}_{ij} = \left.\frac{P_p}{P_b}\right|_{v_{pl}} \tag{4}$$

During blunting, the crack growth is assumed to be very low and both samples behave as blunt specimens. From the constancy of S^{pb}_{ij}, it is possible to determine the early region,

where the load separation condition is not valid, and the point of initiation of crack growing in the precracked experiment when S^{pb}_{ij} starts to drop at a certain level of v_{pl}.

In the range of the load separation validity, the load can be represented as a multiplication of two separate functions, a geometry and a deformation function. For deeply cracked bend-type specimens, the geometry function was calculated previously following the analysis of Rice[12] and was also experimentally confirmed for many polymers[3,14]. Hence, the deformation function or the material key curve can be constructed by normalizing the test records by the geometry function as follows:

$$H(v_{pl}/W) = P/G(b/W) \tag{5}$$

The deformation material function *J-R* curve may be simply developed from a single precracked experiment applying the normalization method.

Normalization procedure

1. A precracked specimen is loaded up to a certain prefixed displacement level after the maximum load allowing the crack to grow considerably (more than approximately 1 mm) but not through the complete remaining ligament (preferably not less than 15 % of the initial remaining ligament) in order to generate a suitable load-displacement record.

2. A blunt-notched specimen is also loaded and the load-displacement curve recorded. It is convenient that the reference blunt-notched specimen curve has a sufficiently deep notch in order to guarantee that the transition to the growing crack regime (load relaxation[14,17]) does not occur in the plastic displacement range of interest[3].

3. Actual initial and final crack lengths, a_o and a_f, are physically determined from the specimen fracture surface of the completely broken samples.

4. Load vs. total displacement records are transformed into load vs. plastic displacement records by calculating the plastic displacement as follows:

$$v_{pl} = v - v_{el} = v - P.C(a/W) \tag{6}$$

where $C(a/W)$ is the elastic compliance. The current elastic compliance value is determined for the initial crack length (a_o) as the slope of the initial linear part of the load-displacement record. From this current value, an effective elastic modulus is calculated using the expression proposed in an ASTM standard[7]. From this modulus and the compliance formula[23], it is possible to estimate the elastic compliance for other crack lengths.

5. The separation parameter S^{pb}_{ij} is evaluated by dividing the load of the growing experiment (precracked specimen) by the load of the stationary experiment (blunt-notched specimen) at different values of constant plastic displacement. The plastic displacement range in which the separation parameter maintains its constancy can be determined.

6. Determination of the deformation function

The deformation function is constructed in the load separation validity zone by normalizing the load by sample dimensions and the geometry function:

$$P_N = \frac{P}{B.W.(b/W)^2} = H(v_{pl}/W) \tag{7}$$

This function can be determined for certain special points or calibration points of the precracked load-displacement records for which a_i is known (item 3).

If we assume only the crack extension due to blunting within the separable blunting zone and that the crack extension follows the analytical expression of the blunting line (which assumed a blunted crack with a semicircular profile), instantaneous values of crack, a_i, may be estimated from

$$a_i = \frac{J}{2\sigma_y} + a_o \tag{8}$$

where σ_y is the yield stress in a tensile experiment. Hence, a_i and P_N can be calculated for the blunting zone. For the final record point (P_{Nf}, $v_{pl\,f}/W$, a_f), P_N can be directly calculated.

The deformation function is developed by regressing those P_N data points to one curve known as the key curve following the fitting procedures recommended in the literature:

(a) Power law function with final point

Assuming a power-law material type behaviour:

$$P_N = \beta.(v_{pl}/W)^n \tag{9}$$

The unknown fitting constants β and n of the power law were obtained by linear fitting log P_N vs. log v_{pl} for the calibration points.

(b) Power law function without including physically determined final point crack growth.

Considering that the start of the deviation from linearity coincides with the start of the real crack advance, the deformation function can be obtained as a simple power law expression by linear fitting log P_N vs. log v_{pl} using only points before the deviation from linearity[14].

(c) LMN function

The LMN function proposed by Orange[24] is given by the following expression:

$$P_N = \frac{[L + M.(v_{pl}/W)].(v_{pl}/W)}{[N + (v_{pl}/W)]} \tag{10}$$

The unknown fitting constants, L, M, and N are determined as follows[4]. L is obtained from the limit load solution in the EPRI Handbook[13] for the single-edge bent specimen:

$$L = \frac{P_L}{G(a_o/W)} \tag{11}$$

$$P_L = 0.364.\sigma_y.B.(W - a_o)^2 \tag{12}$$

and M is obtained as the slope of the straight line $P_N = L + M(v_{pl}/W)$, which is the asymptotic form of the LMN expression obtained by connecting L with the final point in the P_N vs. v_{pl}/W plot. Finally, N is obtained by best fitting the P_N vs. v_{pl}/W plot values at the calibration points to the LMN function.

(d) Combined power law and straight line[15)]

The initial part of P_N vs. v_{pl}/W plot (crack blunting zone) is fitted with a power law for low v_{pl}/W values (partial power law) and then changed to a straight line at some low value of v_{pl}/W including the final point. Actually, the determination of the current transition point between the two functions may need an extra calibration point; however, from a practical point of view, it is assumed to be the one which forms the smallest slope of the straight line connecting the transition point with the final point (the tangent point).

$$P_N = \beta_1.(v_{pl}/W)^{n_1} \qquad \text{for } v_{pl} < v_{pl} \text{ tangent point,} \tag{13}$$

$$P_N = A + B.(v_{pl}/W) \qquad \text{for } v_{pl} > v_{pl} \text{ tangent point} \tag{14}$$

7. Determination of crack length

From the determined functional form of the deformation function $H(v_{pl}/W)$, the plastic displacement v_{pl} is predicted as a function of the normalized load:

$$v_{pl} = f(P_N) \tag{15}$$

and the instantaneous crack length may be calculated iteratively using the instantaneous values of P_i and v_i from the following equations:

$$v_{el} = C(a_i/W)P \tag{16}$$

$$v = v_{el} + v_{pl} \tag{17}$$

8. *J-R* curve construction

The *J-R* curve as $J = 2.U/B.(W-a)$ vs. Δa, can be constructed from the instantaneous values of P_i, v_i and a_i at different plastic displacements. The actual values P_i, v_i and a_i of the final point should always be included in *J-R* calculation in order to check the validity of the numerical predictions.

Experimental

The materials investigated are divided into two groups. The first is composed of several glassy rubber-modified polymers: MIPS, medium-impact rubber-modified polystyrene (Lustrex 2220); HIPS, high-impact rubber-modified polystyrene (Lustrex 4300); ABS, acrylonitrile-butadiene-styrene terpolymer (Lustran ABS HR 850); and RMPMMA, 30%

rubber-modified poly(methyl methacrylate) (Atochem). The other group is formed by two semicrystalline polymers: PP-150, an extrusion-grade isotactic polypropylene, annealed in an oven at 150 °C for 3 h (Cuyolem) and MDPE, a medium-density polyethylene (Finathene). Part of the data used through this paper were first published elsewhere[3,5,25].

Blunt- and sharp-notched specimens were prepared from compression-moulded plates[5,25] and then loaded in the three-point bending mode at room temperature. The thickness-to-depth ratio (B/W) and span-to-depth ratio (S/W) were always kept equal to 0.5 and 4, respectively. PP-150 and RMPMMA-30 samples were 20%-reduced in thickness by side grooving.

MIPS, HIPS, and ABS specimens were loaded at the 2 mm/min crosshead speed while PP-150, MDPE and RMPMMA-30 specimens were loaded at the 1 mm/min crosshead speed. J was determined from the indentation-corrected area under the load-displacement curve. Calibration J-resistance curves were determined by the multiple-specimen technique[23,26].

The yield stress, σ_y, was adopted to be the maximum of the true stress-deformation curve[27]. The yield properties are shown in Table 1. The same σ_y value was adopted for calculations of both the blunting line and limit load.

Table 1. Yield strength, lower limit plastic displacement, normalized final point load and normalized Green and Hundy limit load

Material	σ_y (MPa)	$v_{pl\ min}$ (mm)	Normalized final point load P_{Nf} (N/mm^2)	Normalized Green and Hundy limit load[30] L (N/mm^2)
MIPS	21.9	0.04	12.1	7.4
HIPS	20.6	0.04	11.4	7.7
ABS	38.6	0.02	14.3	7.8
RMPMMA-30	42.7	0.03	12.3	15.5
PP-150	33.0	0.24	14.7	11.8
MDPE	13.7	1.05	11.4	5.0

Results and discussion

Figure 1a shows load-plastic displacement experiments with precracked samples at approximately equal levels of crack growing. In spite of some differences in the shape of the curves related to each type of the behaviour, all materials exhibited nonlinear load-displacement traces and completely stable fracture; the crack grew with a continuous increase in displacement until the complete fracture. Rubber-modified polymers were linear up to a certain load; beyond it, they departed from linearity but the load continued to increase until a

well-defined maximum load was reached. In contrast, the curves displayed by semicrystalline polymers have broad peaks, which are not well defined and reach total displacement levels significantly larger due to the high degree of blunting displayed by these ductile materials.

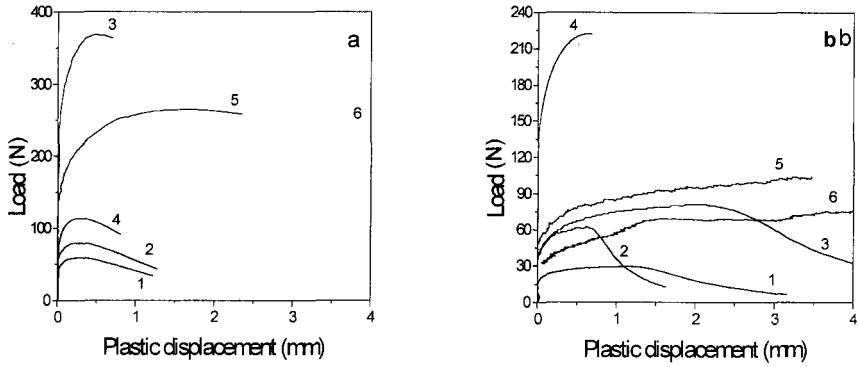

Fig. 1. Load *versus* plastic displacement for (a) precracked specimens, (b) blunt-notched specimens (*1* MIPS, *2* HIPS, *3* ABS HR850, *4* RMPMMA-30, *5* PP-150, *6* MDPE)

Blunt-notched samples (Fig. 1b) of the rubber-modified amorphous polymers (ABS, RMPMMA, MIPS, HIPS) also show a similar trend between load and plastic displacement: the load exhibits an increasing trend with plastic displacement up to a maximum, at which point the load relaxes indicating that the crack has started to propagate and the assumption of the nongrowing crack regime is no longer valid. Semicrystalline polymers (MDPE, PP), however, show a behaviour similar to that reported for metals: the load increases monotonically with displacement without showing any signs of load relaxation[2,22]. These results may provide extra evidence of the statements that support the idea that cracks initiate differently in amorphous and semicrystalline polymers[28].

Figure 2a and b show S_{ij} vs. the plastic displacement plots for all the materials investigated. Consistently with the behaviour explained above, S_{ij} maintains its constancy for larger levels of plastic displacement in the case of semicrystalline materials. These plots reveal the existence of three well defined zones: the inseparable region which is a limited region at the early plastic behaviour, the region where the separation parameter remains constant and the last region where S_{ij} starts to decrease in accord with the crack growth initiation; hence, this point is considered the limit of the crack blunting region. The two former regions correspond to the "blunting zone" of the precracked record where the crack growth is assumed to be very low. Table 1 displays the values of $v_{pl\ min}$ beyond which the use of the J expression is really valid. In fact, the portion of v_{pl} of no validity is small compared with the whole range of v_{pl} (Fig. 2), suggesting that the load separation is a dominant criterion

over the whole range of plastic displacement, and the error in J_{pl} arising from assuming the load separation in the complete range is negligible[29].

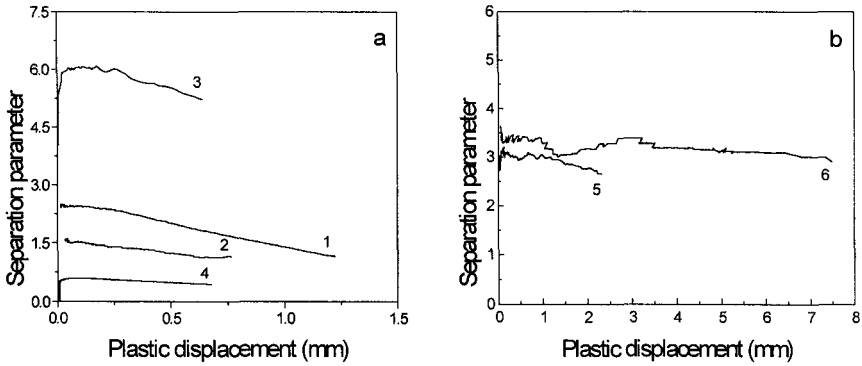

Fig. 2. Separation parameter S_{ij} vs. plastic displacement for (a) rubber-modified, (b) semicrystalline polymers (for curve denotation, see Fig. 1)

Figures 3a-f show the load normalized by the crack length calculated assuming the blunting behaviour and the final point normalized by a_f as a function of v_{pl}/W. The deformation relationships developed in each case and the range of v_{pl} used are shown in the figures. The limit load is also indicated on the plots. Table 1 also compares the load at the final point with the Green and Hundy[30] limit load.

With the sole exception of RMPMMA-30, the normalized load at the final point was always larger than the normalized limit load. Consequently, for this material, the LMN fitting was practically inapplicable. Bernstein also found[8] that for polycarbonate, the maximum load of each load-displacement record was always less than the one predicted by Green and Hundy[30]. He interpreted this result in terms of the start of crack growing before the maximum load is reached, preventing this limit to be reached. We believed that this fact might be related to the lack of definition of the real yield or collapse point for polymers. In metal investigations, the limit load analysis is usually carried out using the yield stress or the effective yield stress[32] as the plastic collapse tension. Even if some authors[4,9,17] adopted this metal criterion as a polymer yield criterion, they did not give a fundamental physical explanation. The latter criterion is not usually taken as the yield stress criterion in polymers, the most diffused one being the maximum load[27,33]. In consequence, for rubber-modified PMMA, the combined power law and the straight line deformation relationship were tried besides the normal power law.

A careful examination of the load-displacement traces (Fig. 3a,b,c,e,f) reveals that the

power law function leads to better regressed key curves than the LMN function. This observation is more evident in the case of semicrystalline polymers.

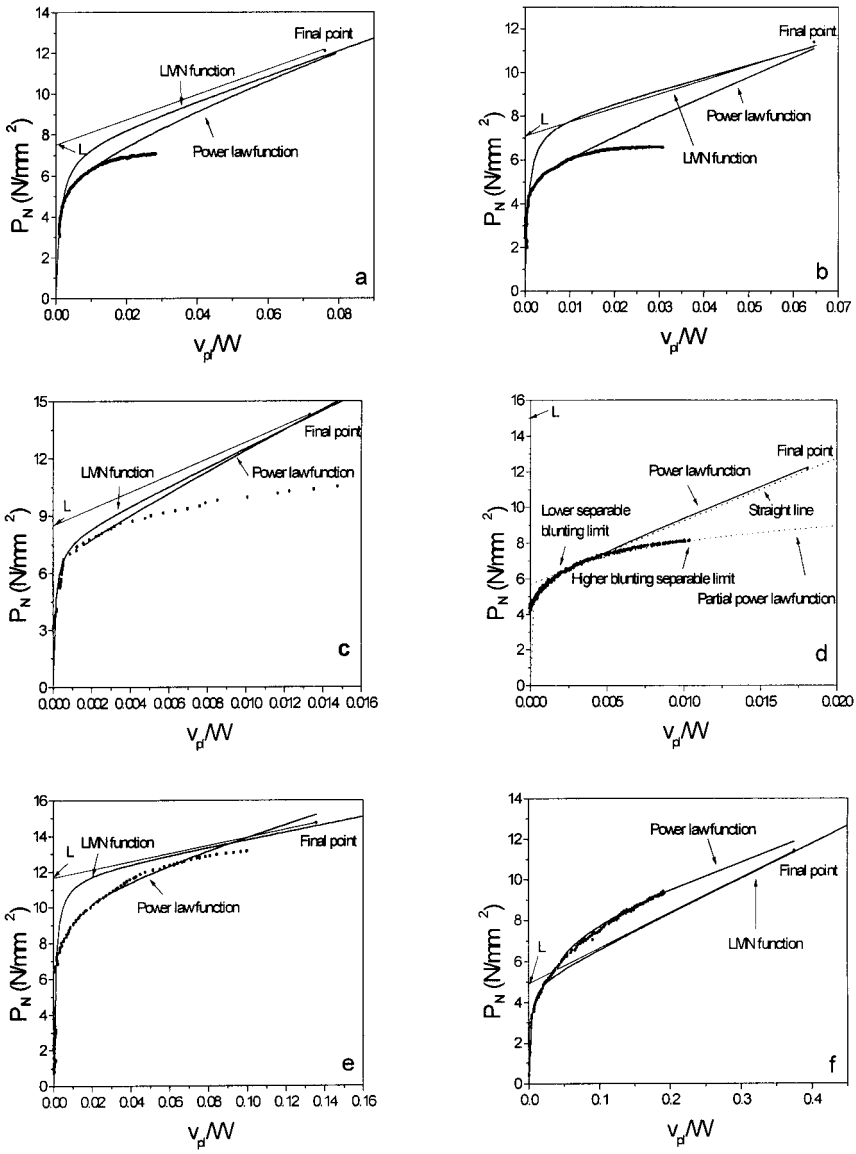

Fig. 3. Normalized load vs. normalized plastic displacement for (a) MIPS, (b) HIPS, (c) ABS, (d) RMPMMA-30, (e) PP-150, (f) MDPE

The LMN function approach results are very dependent on the yield stress of the material whereas with the power law function, the yield stress has a very little influence as it is only

used in the determination of the blunting law. For RMPMMA-30 (Fig. 3d), the power law function and the combined power law and straight line relationship led to similar fittings to the experimental data.

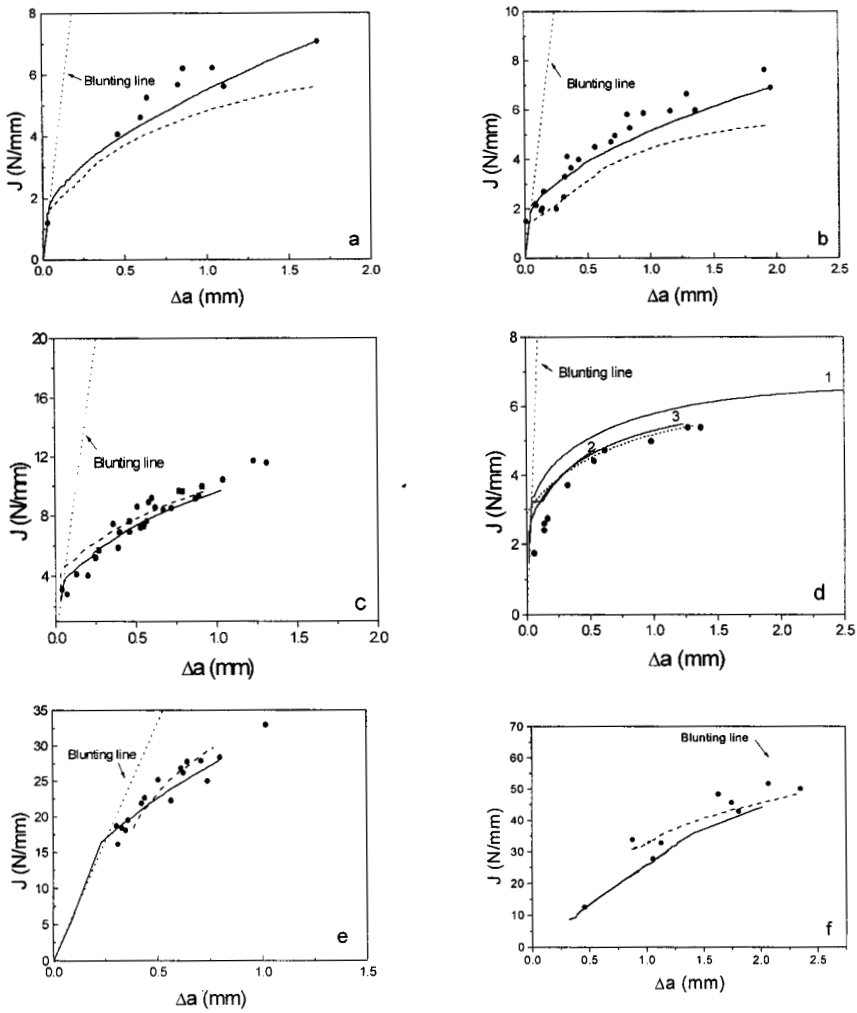

Fig. 4. *J-R* curves obtained by the normalization method with different fitting functions (solid line: power law function, dashed line: LMN function) and by multiple specimen technique (solid points) for (a) MIPS, (b) HIPS, (c) ABS, (d) RMPMMA-30 (*1* without final point, *2* with short final point, *3* with long final point), (e) PP-150, (f) MDPE

Figures 4a-f show the *J-R* curves for the investigated materials obtained using different deformation relationships. Multiple-specimen results are also shown in the same plots.

For rubber-modified polystyrenes (Figs 4a and b), the use of a power law function led

to *J-R* curves that fit better multiple-specimen technique data[3] when compared with the *J-R* curves obtained from the LMN approach.

Normalization method *J-R* curves for ABS (Fig. 4c) obtained by the two routines (power law and LMN functions) were very similar and superimposed the data obtained by the *traditional multiple-specimen technique*[5,26].

Both semicrystalline polymers (Figs 4e and f) displayed better results for the power-law fitting even if both fittings can be considered as good approaches.

Even if it has been reported that the conventional blunting line does not adequately reflect the blunting mechanisms for all polymers[34-36], our *J-R* curves show that most of the materials for practical purposes follow this blunting behaviour (Fig. 4a-f); the introduction of apparent crack growth by blunting appears to be very important since it improves the *J-R* curves with respect to that obtained previously assuming no propagation during blunting[26].

The reproducibility and the dependence of *J-R* curves obtained by the single-specimen technique were examined on RMPMMA-30 by fitting two separate specimens having essentially different crack extensions (Fig. 4d). The shortest crack extension falls in the permitted zone of the ESIS protocol exclusion lines[37]. The *J-R* curves obtained from both specimens matched. As expectable, the longest crack extension offers more information on the material. It was previously stated that protocol exclusion lines are too restrictive for polymers; in fact, using the load separation, it was demonstrated that the validity of *J-R* curves may be extended to longer v_{pl} levels[3,5,26].

The RMPMMA-30 deformation function was also fitted using the power law function without final point to make evident the importance of forcing the fitting to include the final point. The incorporation of the final point really improves the fitting (Fig. 4d). However, the interest in this approach, which does not include the final point, is based on the fact that in some cases, the determination of the final point is not easy, such as under impact conditions or because it does not appear evident from the analysis of the fractured surface[38].

Conclusions

Several normalization procedures differing in the fitting of the deformation function were assessed in order to determine *J-R* curves for several ductile polymers: the power law function, the LMN function, and a combined power law and linear fitting approach. The approaches are simple to apply from both experimental and mathematical points of view. However, the power law approach is the simplest as a fitting technique. The LMN equation appears to be dependent on the plastic collapse tension which is a function of σ_y, not always very easy to predict in polymers due to the lack of a real plastic collapse definition. This

uncertainty may lead to troubles in the determination of the L and M constants.

The most appropriate deformation relationship may be determined from a careful study of the material deformation pattern (the shape of normalized load vs. the plastic displacement plot); hence, the function that leads to a better fitting of the data should be chosen.

Virtually all deformation relationships assessed led to *J-R* curves that are in reasonably good agreement with those obtained by the multiple-specimen technique even if some differences were detected in the fitted key curves.

The inclusion of the apparent crack tip blunting growth and the final point in the fitting of the deformation function improves the resulting *J-R* curves.

Of the results shown here, the method of normalization, which allows to develop *J-R* curves from load-displacement records, has an advantage over the commonly used multiple-specimen technique and seems to be applicable to many polymers. Further work is in progress to adapt this methodology to the dynamic *J-R* curve determination[35].

Acknowledgements

The authors would like to thank CONICET and CNR for financial support.

Symbols

J	*J*-integral	A	area under the load-displacement record
J_{IC}	plane strain fracture toughness	C	elastic compliance
b	uncracked ligament	K	stress intensity factor
U	potential energy of the loaded body	E	Young's modulus
a	crack length	W	specimen width
v	displacement	S	separation parameter
P	load	η	geometry factor used to calculate the *J*-integral from the energy U
P_L	limit load	σ_y	yield stress
G	geometry function	H_{pb}	ratio of the deformation functions for precracked and blunt-notched specimens
H	material deformation function		

Subscripts

el, pl	elastic and plastic components, resp.	b	blunt-notched specimen
p	precracked specimen		

References

1. ASTM E1152-87: Standard test method for determining J-R curves. *Annual Book of Standards*, Part 10. ASTM, Philadelphia, PA, 1987
2. M.H. Sharobeam, J.D. Landes, *Int. J. Fracture* **47**, 81 (1991)
3. C.R. Bernal, P.E. Montemartini, P.M. Frontini, *J. Polym. Sci., Part B: Polym. Phys.* **34**, 1869 (1996)
4. J.D. Landes, Z. Zhou, *Int. J. Fract.* **63**, 383 (1993)
5. C.R. Bernal, A.N. Cassanelli, P.M. Frontini, *Polym. Test.* **14**, 85 (1995)
6. M. Che, W. Grellmann, S. Seidler, J.D. Landes. *Fatigue Fract. Eng. Mater. Struct.* **20**, 119

(1997)
7. N. Okumra, T.V. Venkatasubramanian, B.A. Unvala, T.J. Baker, *Eng. Fract. Mech.* **14**, 617 (1981)
8. S. Hashemi, J.G. Williams, *Polym. Eng. Sci.* **26**, 760 (1986)
9. W.N. Chung, J.G. Williams, in *Elastic-Plastic Fracture Test Methods: The User's Experience* (Vol. 2), ASTM STP 1114, ASTM, Philadelphia, PA, 1991, p. 320
10. H.A. Ernst, P.C. Paris, M. Rossow, J.W. Hutchinson, in *Fracture Mechanics*, ASTM STP 677, ASTM, Philadelphia, 1979, p. 581
11. H.A. Ernst, P.C. Paris, J.D. Landes, in *Fracture Mechanics,* 13th Conference, ASTM STP 743, ASTM, Philadelphia, PA,1981, p. 476
12. J.R. Rice, *J. Appl. Mech.* **35**, 379 (1968)
13. V. Kumar, M.D. German, C.F. Shih, *An Engineering Approach for Elastic-Plastic Fracture Analysis*, EPRI Report NP-1931, (1981)
14. C.R. Bernal, A.N. Cassanelli, P.M. Frontini, *Polymer* **37**, 4033 (1996)
15. R. Herrera, J.D. Landes, in *Fracture Mechanics,* 21st Symposium, ASTM STP 1074, ASTM, Philadelphia, PA, 1990, p. 24
16. A.N. Cassanelli, L.A. de Vedia, *Int. J. Fract.* **83**, 167 (1997)
17. Z. Zhou, J.D. Landes, D.D. Huang, *Polym. Eng. Sci.* **34**, 128 (1994)
18. J.D. Landes, Z. Zhou, K. Lee, R. Herrera, *J. Test. Eval.* **19**, 305 (1991)
19. J.R. Begley, J.D. Landes, in *Fracture Toughness*, ASTM STP 514, ASTM, Philadelphia, PA, 1972, p. 1
20. J.D.G. Sumpter, C.E. Turner, in *Cracks and Fracture*, ASTM STP 601, ASTM, Philadelphia, PA, 1976, p. 3
21. L.A. de Vedia, in *Mecánica de Fracturas*, Proyecto Multinacional de Investigación y Desarrollo de Materiales OEA-CNEA, Buenos Aires, 1986.
22. M.H. Sharobeam, J.D. Landes, *Int. J. Fract.* **59**, 213 (1993)
23. ASTM E813-87: Standard test method for JIC, a measure of fracture toughness, 1987. *Annual Book of ASTM Standards*, Part 10. ASTM, Philadelphia, PA, 1987, p. 968
24. T.W. Orange, *Fracture Mechanics,* 21st Symposium, ASTM STP 1074, ASTM, Philadelphia, PA, 1990, p. 545
25. P.M. Frontini, A. Fave, *J. Mater. Sci.* **30**, 2446 (1995)
26. C. Bernal, P.M. Frontini, R. Herrera. *Polym. Test.* **11**, 271 (1992)
27. R.N. Haward, *The Physics of Glassy Polymers*, Applied Science Publishers, London 1973, p. 285
28. S. Seidler, W. Grellmann, in Proc. 8th Int. Conf. *Deformation, Yield and Fracture of Polymers*, Cambridge, 1997, p. 40/1
29. M. Sharobeam, J.D. Landes, in *Fracture Mechanics*, 22nd Symposium (Vol. I), ASTM STP 1131, ASTM, Philadelphia, PA, 1992, p. 198
30. A.P. Green, B.B. Hundy, *J. Mech. Phys. Solids* **4**, 1956
31. H.L. Bernstein, in *Elastic-Plastic Fracture Tests Methods: The User's Experience* (Vol. 2), ASTM STP 1140, ASTM, Philadelphia, PA,1990, p. 306
32. J.D. Landes, K.H. Brown , R. Herrera in *Fracture Mechanics,* 22nd Symposium (Vol. I), ASTM STP 1131, ASTM, Philadelphia, PA, 1992, p.158
33. M.D. Wang, E. Nakanishi, Y. Hashizuma, S. Hibi, *Polymer* **33**, 2715 (1992)
34. S. Hashemi, J.D. Williams, *Polymer* **27**, 384 (1986)
35. M.K.V. Chan, J.D. Williams, *Int. J. Fract.* **19**, 145 (1983)
36. M.T. Takemori, Y. Narisawa, in *7th Int. Conf. on Fracture* Houston, 1989, p. 2733
37. G. Hale, *A Testing Protocol for Conducting J-Crack Growth Resistance Curve Tests on Plastics*, ESIS, 1995
38. L. Fasce, C. Bernal, G. Carcagno, P. Frontini, H. Sautereau, in Proc. 8th Int. Conf. *Deformation, Yield and Fracture of Polymers*, Cambridge, 1997, p. 250